Original article

Journal of High School Science

Evaluating macroscopic traffic flow models using real vehicle trajectory data

Park L

Submitted: April 18, 2024, Revised: version 1, July 15, 2024, version 2, October 15, 2024, version 3, November 14, 2024
Accepted: November 17, 2024

Abstract
Increasing urban highway traffic and congestion require more effective methods to understand and predict traffic flows. This paper evaluated two macroscopic traffic flow models by using the models to predict the flow of traffic along a stretch of the US 101 highway in Los Angeles, California, a dense urban area. A data set of vehicle trajectory observations for three time periods of different traffic phases was used to calibrate, simulate, and analyze the models. Both macroscopic models were constructed using an ordinary differential equation that models the flow of vehicles as continuous variables. The models utilized the Greenshields and Daganzo-Newell traffic flux functions. First, observational data from the highway was used to calculate various variables, some of which were used to estimate parameters for the two traffic flux functions. Other measured variables were utilized to numerically simulate the volume, the number of vehicles, using the models' predictions. The difference between the predicted and observed volumes were used to evaluate the predictive accuracy of the models. Both instantaneous error and average error functions were defined to quantitatively measure a model's predictive accuracy for a simulation. Each model was simulated in two different scenarios. The first scenario was for the entire duration of time for which the observational data was available. The second scenario excluded the first minute, a period of time where observational data was incomplete. The Daganzo-Newell model consistently performed better with less errors. It was more accurate than the Greenshields model in both simulations, and achieved the lowest average error in the second simulation. The Greenshields model's performance did not vary significantly between the two simulations.

Keywords
Traffic flow, Macroscopic model, Ordinary Differential Equation, Numerical simulation, Mathematical modeling, Time series analysis, Greenshields traffic flux function, Daganzo-Newell traffic flux function, Highway congestion

Lauren Park, Mountain View High School, 3535 Truman Avenue, Mountain View, CA 94040, USA. lauren.park.math@gmail.com

Introduction

Transportation is integral to urban life. The connection between residents, businesses, goods, and services facilitates the communication and collaboration of a city. As urban traffic and congestion continue to grow, highways cannot simply be expanded to accommodate increased traffic. Thus, congestion relief must primarily come from effective highway operations (1). A key to developing relief methods is to predict traffic flow through modeling. Mathematical modeling can be an effective tool for understanding and optimizing traffic flows in order to create more efficient transportation systems. Discovering accurate models is the first step in developing better traffic control policies, and urban planning.

Macroscopic traffic flow models

There are two basic types of traffic flow models: microscopic models and macroscopic models. Microscopic models focus on the actions and interactions between individual vehicles, and tend to be more complex and challenging to use for practical applications, such as predicting the flow of traffic. On the other hand, macroscopic models are more computationally efficient because they treat traffic as a continuous fluid flow. Macroscopic models are more straightforward to use as predictors if the inputs into the models are readily observed variables. However, they also utilize assumptions that can lead to inaccuracies under certain conditions.

Macroscopic modeling of traffic flows starts with an idealized stretch of straight single lane road on which all vehicles travel along from the left to the right. Vehicles enter the start of the road on the left and exit the end of the road on the right.

Figure 1. An instantaneous snapshot of vehicles entering and exiting a road at time t. Arrows indicate the magnitude of a vehicle's velocity.

Macroscopic models assume the conservation of vehicles: all vehicles entering a road, exit the road. The second assumption is that the motion of individual vehicles can be aggregated into a continuous fluid-like flow along the road. Just like vehicles can move at different velocities, the flow can also move at different velocities.

Additionally, the flow has a density, the number of vehicles along the length of the flow. Combining these ideas, a flow's density and velocity can vary continuously across time and location along the road. This intuition is formally captured in the following partial differential equation (PDE) and identity relationship

$$\frac{\partial k}{\partial t} + \frac{\partial q}{\partial x} = 0, q = vk$$

Where k is density (vehicles/distance), q is flow (vehicles/time)—the number of vehicles passing a position x per unit time, and v is velocity (distance/time) at time t and position x (distance).

Based on the above, changes in flow along the road are propagated through changes in density of vehicles through time to preserve the conservation of vehicles law. The model has two variables but only one equation. Thus, a way to transform the equation to one variable is required.

The Lighthill-Whitham-Richards (LWR) model is an early macroscopic model that was influential to the field of traffic flow modeling. The LWR model (2, 3) relies upon a functional relationship between k and v that is observed in traffic data

$$v = V(k)$$

This then allows q to be modeled as

$$Q(k) = kV(k).$$

$Q(k)$ is commonly referred to as the traffic flux function. The determination of $Q(k)$ is critical to a traffic flow model since it captures the dynamic relationship between k and v. Thus the LWR model becomes a PDE of a single variable

$$\frac{\partial k}{\partial t} + \frac{\partial}{\partial x}\big(Q(k)\big) = 0 \quad \text{or} \quad \frac{\partial k}{\partial t} + \frac{\partial}{\partial x}\big(kV(k)\big) = 0, \text{ and } k(x,0) = f(x), k(0,t) = g(t).$$

$k(x, 0)$ is the initial condition, the density of vehicles along the road at $t = 0$. $k(0, t) = g(t)$ is the boundary condition, the time varying density of vehicles entering the road. The solution to the PDE, $k(x, t)$, calculates the density along the stretch of road and how it varies in time and location.

In this manuscript, when a variable is written in lowercase, e.g., v, representing the flow velocity, it indicates that the variable is directly empirically observed or calculated. When a variable is written in uppercase, e.g., V, also representing the flow velocity, it indicates that the variable is being calculated as a function of another empirically observed variable. This notation convention applies to all variables, except N, the volume or the number of vehicles on the road. N is the variable that our model is predicting, but it also can be directly measured from the data. The empirically observed N is referenced as $empirical\, N$. The model predicted N is referenced as $predicted\, N$. N referenced with no prefix refers to both types of N.

Derivation of the ODE model

Due to the complexities of numerically solving the LWR model (4), which is a PDE, this paper aims to analyze the accuracy of a simpler traffic flow model from Mark McCartney and Malachy Carey (5). The McCartney-Carey model assumes that the rate of outflow from a stretch of road, L long, is a function of the volume. This model does not describe the internal structure of the road as the LWR model does. Rather the McCartney-Carey model treats the entire stretch of road as a single uniform whole. Since volume is assumed to be conserved—if a vehicle enters the road, it will exit the road—the rate of change of the volume is the inflow minus the outflow, or (eq1), (eq1b),

$$\frac{dN}{dt} = u(t) - Q(N) \qquad \text{(eq1)}$$
$$k = N(t)/L \qquad \text{(eq1a)}$$
$$q = vk \qquad \text{(eq1b)}$$

where N is the volume at time t, $u(t)$ is the inflow of vehicles (vehicles/time), and $Q(N)$ is the outflow of vehicles (vehicles/time). The function $u(t)$ acts as a boundary condition for the model. The function $Q(N)$, commonly referred to as the "flux function", is a key element of the McCartney-Carey model, and should be of physically realistic form.

For example, $Q(N)$ should tend towards zero as N approaches zero – if there are fewer vehicles on the road, then fewer vehicles should be leaving the road. $Q(N)$ should also tend towards zero as N increases – eventually if there are too many vehicles on the road, traffic will jam and the number of vehicles leaving the road will tend towards zero. Given the fixed relationship between N and k, $Q(N)$ can be written in terms of k, i.e., $Q(k)$. There are many different types of $Q(k)$ (6-10). Each is motivated by different aspects of the observed relationships between k, v or q. Selecting different $Q(k)$ allows the development of different traffic models for a particular road. For this investigation two flux functions were chosen. Our first model uses a $Q(k)$ commonly referred to as the Greenshields flux function (6, 9). We start with $Q(k)$ to be the product of k, the average density of vehicles per unit distance, and v, the average velocity of the vehicles (distance per unit time) on the road at time t, (eq2).

$$Q(k) = k(t)v(t) \quad \text{(eq2)}$$

The relationship between traffic density and vehicle velocity is well established in traffic research. Our first model estimates the relationship between density and velocity as a linear function to calculate velocity as a function of density, (eq2a).

$$Q(k) = k(t)V\big(k(t)\big) \quad \text{(eq2a)}$$

Our second model uses the piecewise linear Daganzo-Newell flux function (7 - 9) (eq3).

$$Q(k) = \begin{cases} Q_{max}\frac{k}{k_c} & \text{for } 0 \leq k \leq k_c \\ Q_{max}\frac{k_{max}-k}{k_{max}-k_c} & \text{for } k_c \leq k \leq k_{max} \end{cases} \quad \text{(eq3)}$$

This flux function directly estimates the relationship between q and k that is observed in traffic flow data. Observations of traffic flow show that for density up to a critical density, k_c, the outflow increases linearly. Outflow then generally decreases with a wide dispersion until a maximum density, k_{max}. Each model is built upon equation 1, an ordinary differential equation (ODE), with $u(t)$ calculated from empirical data. Thus, the models are (eq4), (eq4a), (eq4b). $empirical\ N(0)$ is the actual observed volume of vehicles in the road at $t = 0$.

$$\frac{dN}{dt} = u(t) - Q(k) \quad \text{(eq4)}$$

$$k(t) = N(t)/L \quad \text{(eq4a)}$$

$$N(0) = empirical\ N(0) \quad \text{(eq4b)}$$

General approach

To use differential equation 4 to predict traffic flow, empirical data for a highway (11) was first utilized to estimate the parameters for a model's flux function, $Q(k)$.

For the Greenshields flux function, the empirical data was used to calculate the average velocity and average density of the study area during the observation period. The calculated values were used to make the fundamental diagram (FD) of traffic flow. For the Greenshields flux function, the FD was a scatter plot of v vs k. A line of best fit was calculated for velocity as a function of density. Substituting the equation of the line into equation 4 resulted in $Q(k)$ having a quadratic form, the Greenshields flux function (6). For the Daganzo-Newell flux function (7, 8), the empirical data was used to calculate the average outflow and average density of the study area during the observation period. The calculated values were used to make the FD which is a scatter plot of q vs k. Instead of attempting to directly estimate the values for the parameters in equation 3, we selected a function that approximated equation 3 and which could be fitted to the empirical data. As in (12) we used the function Q(k) of equation 5 (eq5).

$$Q(k) = \alpha\left(a + (b-a)\frac{k}{k_{max}} - \sqrt{1+y^2}\right), \qquad \text{(eq5)}$$

where $a = \sqrt{1+(\lambda p)^2}$, $b = \sqrt{1+\left(\lambda(1-p)\right)^2}$, and $y = \lambda\left(\frac{k}{k_{max}} - p\right)$

Equation 5 approximates equation 3 very well. The parameter p allows for control of k_{max} , the density at which traffic flow stops. The parameter α controls Q_{max}, the maximum predicted outflow rate. The parameter λ controls the "sharpness" or "roundedness" of the transition between the two linear segments of equation 3. Note that $Q(0) = 0$ and $Q(k_{max}) = 0$. Since the study area was of fixed length, dividing $N(t)$ by L provided $k(t)$. Using Greenshields $Q(k)$ or Daganzo-Newell $Q(k)$, it is straightforward to calculate the predicted outflow given volume. Next, $u(t)$ and $empirical\ N(t)$ were calculated from the empirical data. Finally, the value of $empirical\ N(t)$ at $t = 0$ was used as the initial value of $predicted\ N(t)$. Subsequently, equation 4 could be numerically integrated to calculate $predicted\ N(t)$. Finally, to analyze the accuracy of our traffic flow models, the $predicted\ N(t)$ is compared to the $empirical\ N(t)$.

Materials and Methods

The Dataset

The empirical data for this paper was from a publicly available dataset recorded by the U.S. Department of Transportation (DOT) for the Next Generation Simulation (NGSIM) program (11). The NGSIM description of the generation of the data set quotes "Researchers for the NGSIM program collected detailed vehicle trajectory data on southbound US 101, also known as the Hollywood Freeway, in Los Angeles, CA, on June 15th, 2005. The study area was approximately 640 meters (2,100 feet) in length and consisted of five mainline lanes throughout the section. An auxiliary lane is present through a portion of the corridor between the on-ramp at Ventura Boulevard and the off-ramp at Cahuenga Boulevard. Eight synchronized digital video cameras, mounted from the top of a 36-story building adjacent to the freeway, recorded vehicles passing through the study area. NGVIDEO, a customized software application developed for the NGSIM program, transcribed the vehicle trajectory data from the video. This vehicle trajectory data provided the precise location of each vehicle within the study area every one-tenth of a second, resulting in detailed lane positions and locations relative to other vehicles. A total of 45 minutes of data are available in the full dataset, segmented into three 15 minute periods: 7:50 a.m. to 8:05 a.m.; 8:05 a.m. to 8:20 a.m.; and 8:20 a.m. to 8:35 a.m. These periods represent the buildup of congestion, or the transition between uncongested and congested conditions, and full congestion during the peak period." Figure 2, adapted from one of the NGSIM documents (11), depicts the study area. The raw data from the NGSIM contained duplicate records, hence this paper used a cleaned data set prepared by Cambridge Systematics, Inc. with the duplicates removed. The cleaned data set is also available from the NGSIM website (11).

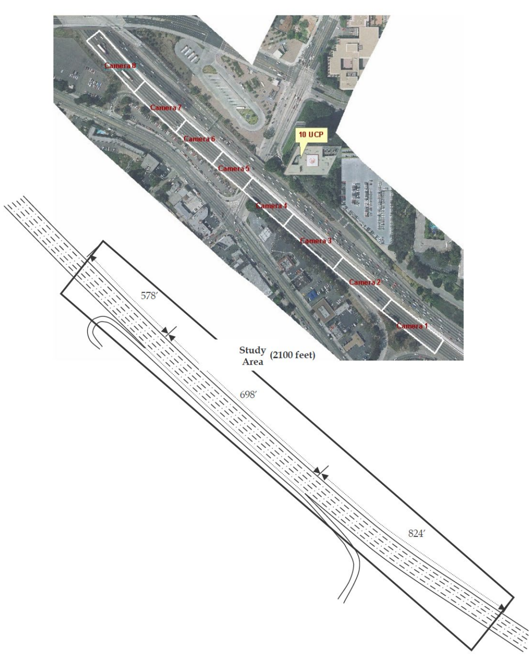

Figure 2. Study Area Schematic and Camera Coverage. The study area is 640 meters long.

Each row in the dataset is an instantaneous observation of one vehicle at a specific time. The dataset includes the vehicle identification number of the vehicle, the elapsed time in milliseconds since January 1, 1970, the local x and y coordinates, the length of the vehicle, the width of the vehicle, the instantaneous velocity, the instantaneous acceleration, the lane that the vehicle is in, the vehicle identification numbers of the preceding and following vehicles, the space headway, and the time headway, among other values.

Data Preparation

The data set of 4,098,933 observation records was loaded into a table in a MySQL relational database. SQL (Standard Query Language) was utilized to perform data aggregations and calculations. The data set was checked to ensure that there were no duplicate records for observed vehicles. The slowest recorded instantaneous velocity was 0 meters per second (mps) and the fastest recorded instantaneous velocity was 29.05 mps (95.30 feet per second) or 104.57 kilometers per hour (kph) (64.98 miles per hour). There were 6,046 distinct vehicles observed during the observation time period.

Our model, equation 4, is a macroscopic traffic flow model which aggregates the behavior of individual vehicles into instantaneous flows across distance and time. This raised the question of how to aggregate individual vehicle observations into a continuous flow. Additionally, in order to solve our model practically, it was necessary to select time scales and distance scales for calculating model variable values. From analysis of the data set, we selected appropriate lengths for intervals for time and distance, i.e., bin size. Values for a bin were actually averages over the bin's interval. The model variables that need to be averaged across time and distance bins were $k(t), v(t), u(t),$ $q(t)$, $empirical\, N(t)$, and $predicted\, N(t)$. In the data set, lanes 1, 2, 3, 4, and 5 are the mainline lanes that extend through the entire study area. The auxiliary lane, on-ramp, and off-ramp are lanes 6, 7, and 8, respectively.

An immediate question was to determine if or how the on-ramp, auxiliary lane, and off-ramp should be incorporated into the model. The data set was analyzed to count exactly how many vehicles entered and exited the study area. 5,429 vehicles entered and exited via the mainline lanes. 219 vehicles entered via the mainline lanes and exited via the off-ramp. 398 entered via the on-ramp and exited via the mainline lanes. 3 entered the on-ramp and exited the off-ramp. Hence, 179 net vehicles were added to the mainline lanes via the on-ramp, which is only 3.3% of vehicles entering and exiting via the mainline lanes, which would not be significant in calculations involving the mainline lanes. Thus, we decided to ignore the data from the on-ramp, auxiliary lane, and off-ramp in our modeling. (Note also that the on-ramp, auxiliary lane and off-ramp are significantly less than 640 m long.) The first consequence was related to $u(t)$. The total number of cars entering the study area decreased by 179 vehicles. The second consequence was related to $q(t)$. The total number of cars leaving increased by 179 vehicles. There was no impact to $v(t)$ and $k(t)$. All observations of vehicles in the mainline lanes were included in the calculations of these functions regardless of how they entered or exited the study area. For the time scale, except for $q(t)$, all values were calculated over one second time intervals. Essentially, records in the data set were "binned" into one second and then averaged to calculate aggregate values. Thus, the 45 minute observation period was divided into 2,700 seconds. A one second interval was chosen based upon two considerations. First, there were a sufficient number of observations for each one second interval to calculate averages. Except for the last 30 seconds of the observation period, all time intervals contained more than 400 observations. Across the entire dataset there was an average of 1,480 observations per second. Second, the one second interval would allow for the simulation of the model to generate sufficient predictions across the three phases of traffic during the observation period so that the model's predictions could be evaluated against the empirical data.

The one second time intervals were measured in bins that started at 7:50:00 AM. Thus t = 61 represented the one second long bin that started at 7:51:01 AM. $v(t)$, the average velocity of vehicles in the study area was calculated as a mean time velocity by assigning each observation to a one second bin and then dividing by the total number of observations in the bin. $empirical\ N(t)$ was calculated by assigning each observation to a one second bin and then dividing by the maximum number of possible observations for a vehicle in the bin. A vehicle was filmed at a frequency of 10 times a second, which means that if there were 10 observations of a vehicle in a second, there was one vehicle in that one second bin. Thus, there could be fractional counts for a vehicle in a one second bin. This occurs when a vehicle entered or exited the study area during a one second bin. $k(t)$, the average density of vehicles in the study area was calculated by dividing $empirical\ N(t)$ by L = 640 m. $u(t)$, the rate of vehicles entering the area was measured using the earliest time that a vehicle was observed entering lanes 1, 2, 3, 4, or 5. The total number of vehicles entering during a 1 second time bin was divided by the length of the time bin (1 second) to obtain inflow as a function of time. $q(t)$, the rate of vehicles exiting the study area, was measured as the earliest time that a vehicle was observed as having traveled past L in lanes 1, 2, 3, 4, or 5. $k(t)$ and $v(t)$ averaged over one second bins were used to calibrate the Greenshields flux function. However, $k(t)$ and $q(t)$ averaged over ten second time bins were used to calibrate the Daganzo-Newell flux function. $q(t)$ averaged over one second time bins were too "noisy" to fit equation 5. There were too many instances, (223 / 2700 observations or 8.26%), where $q(t)$ averaged over one second was 0. Given the ways that $k(t), v(t), u(t)$, $q(t)$, and $empirical\ N(t)$ were measured, they are all step functions.

Calibration of the Greenshields Flux function

Using Python, a scatter plot of velocity, $v(t)$ vs density, $k(t)$ was constructed with Matplotlib and NumPy, extreme outliers were removed, and a line of best fit was determined using scikit-learn using the least squares method. From equation 2 and equation 2a, outflow (vehicles per unit time) is the product of density and velocity. This leads to outflow as a function of density. Thus, our model assumed that the density and velocity of the flow were uniform across the study area. Thus, volume could be simply calculated as density times L = 640 m (2,100 ft), which provided outflow as a function of volume.

Calibration of the Daganzo-Newell flux function

Using Python, a scatter plot of $q(t)$ vs $k(t)$ was plotted with Matplotlib and NumPy, and equation 5 was fitted using SciPy.curve_fit( ), which uses a nonlinear least squares method to find the curve of best fit. This curve described outflow as a function of density. This model also assumed that the density and velocity of the flow were uniform across the study area.

Numerical simulation

Once each model's flux function was calibrated, the differential equation 4 could be simulated using Python's SciPy.solve_ivp( ) to calculate $predicted\ N(t)$ over time. solve_ivp() numerically integrated an ODE given the initial value of the function. The initial condition, the value of $predicted\ N(t)$ at the start time of the simulation was taken from the $empirical\ N(t)$.

Results

Figures 3 and 4 show $v(t)$ and $k(t)$ respectively, which demonstrated, the fundamental inverse relationship between average velocity and average density.

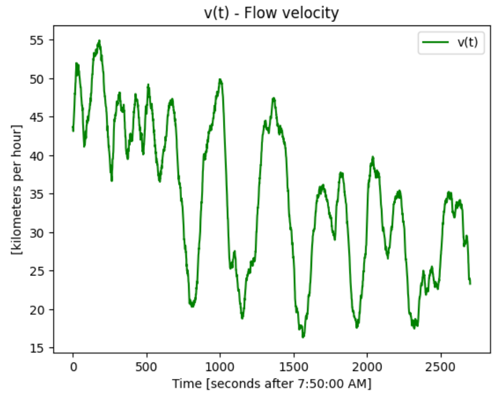

Figure 3. $v(t)$, the flow velocity, the average velocity of vehicles over 1 second intervals.

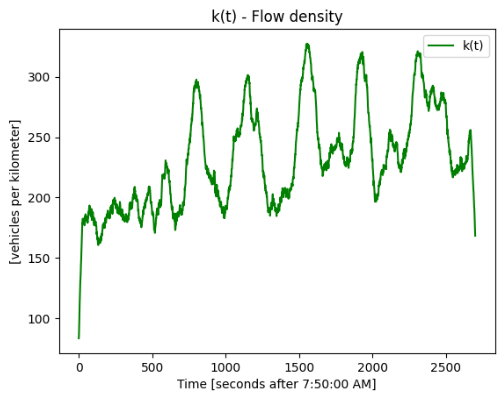

Figure 4. $k(t)$, the flow density, the average density of vehicles over 1 second intervals.

Greenshields Flux Function

Figure 5 shows the velocity v as a function of density k with a line of best fit.

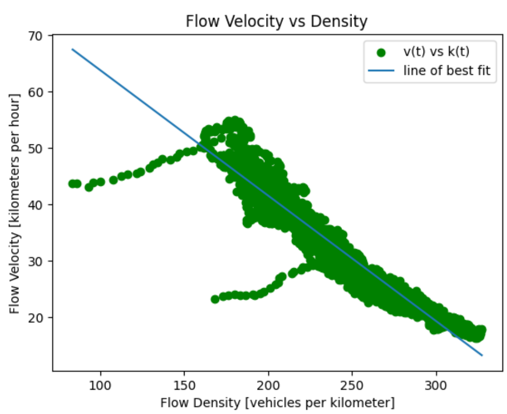

Figure 5. Relationship of $v(t)$ and $k(t)$.

For the purposes of estimating equation 2a, it was decided to remove outliers. Upon detailed examination of the data, the outliers were identified as observations from the start and the end of the data collection time period: the time immediately after 7:50:00 AM and the time immediately before 8:35:00 AM. The observations from 7:50:00 AM to 7:50:59 AM and 8:34:01 to 8:35:00 AM were removed. The empirical data from the beginning and end of the data collection time period are materially different due to the way that observations were made. At the start of the data collection period, there were vehicles already in the study area—vehicles that had entered the study area prior to 7:50:00 AM—but were not tracked and included in the data set. Similarly, because tracking ended at 8:35:00 AM, there were again vehicles that were not tracked because these vehicles exited the study area after 8:35:00 AM.

After excluding these outliers, the remaining observations were used to perform a linear regression to fit a line relating $v(t)$ to $k(t)$. Generally, the slight curve of the distribution of the points for our data set was consistent with that of more complex road networks as reported in Figure 1e of (13). The linearly regressed line was calculated as (eq6) (Figure 6).

$$v(t) = -0.23k(t) + 87.9794 \quad \text{(eq6)}$$

With $R^2 = 0.9316$, a linear model was deemed to be sufficiently accurate. Thus, according to the line of best fit, the maximum average velocity was calculated as 87.98 kph (54.67 mph), which is when density was zero. This occurred when there are very few vehicles on the road, so the flow of vehicles was unimpeded. The maximum density, k_{max}, was 382.53 vehicles per kilometer (615.62 vehicles per mile), which is when the velocity was zero. This occurred when there were so many vehicles on the road that the vehicles were stopped. This implied that the maximum limit to the volume of vehicles in the study area was 244.85 vehicles, which was calculated from the maximum density times the length of the road. Empirically, the greatest number of vehicles in the study area was 211.5 vehicles at $t = 1{,}553$ seconds.

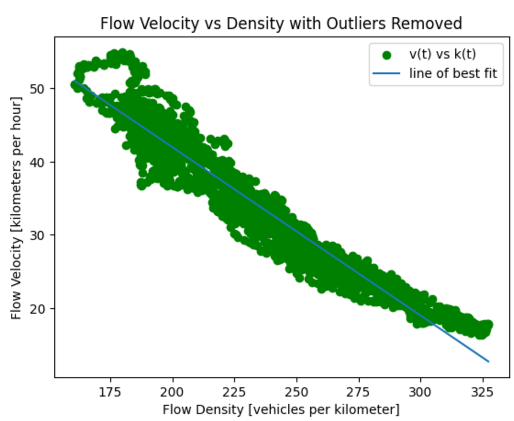

Figure 6. Relationship of $v(t)$ and $k(t)$ with outlier observations in [7:50:00 - 7:50:59, 8:34:31 - 8:35:00] removed.

Substituting equation 6 into equation 3, (eq7), a Greenshields flux function. Values for outflow $Q(k)$ could now be calculated and plotted (Figure 7). For computational purposes, when the density was greater than k_{max}, the outflow rate was set to zero.

$$Q(k) = k(t)(-0.23k(t) + 87.9794) \quad \text{(eq7)}$$

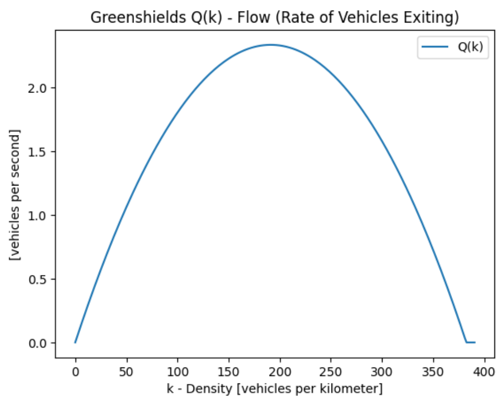

Figure 7. $Q(k)$, the Greenshields flux function. Q_{max} is 2.34 vehicles per sec when k is 191.27 vehicles per km.

Daganzo-Newell Flux Function

For calibrating the parameter values α, λ, and p of equation 5, a time interval of 10 seconds was used for $q(t)$. This was due to the "noisiness" of $q(t)$ at 1 second time interval. There were many intervals where no cars exited the road. The 10 second interval was the smallest time interval where there were vehicles consistently exiting. This provides sufficient data points to fit (5). Also, a value for k_{max} needed to be determined. The k_{max} inferred from the Greenshields flux function was too low (explained in the Discussion section).

We decided to estimate k_{max} in a manner similar to (12) based upon physical restrictions of the road and vehicles. The average vehicle length from the data set was 4.6425 m (15.2321 ft) long. Assuming that a driver will maintain a minimum safety distance of half a vehicle length, the minimum distance for a car stopped on the road is 6.9638 m (22.8482 ft). Thus, k_{max} = 5 lanes / 6.9638 m per vehicle = 0.7180 vehicles / m = 718 vehicles / km. Figures 8 and 9 show $q(t)$ and $k(t)$ respectively, which were used to fit equation 5.

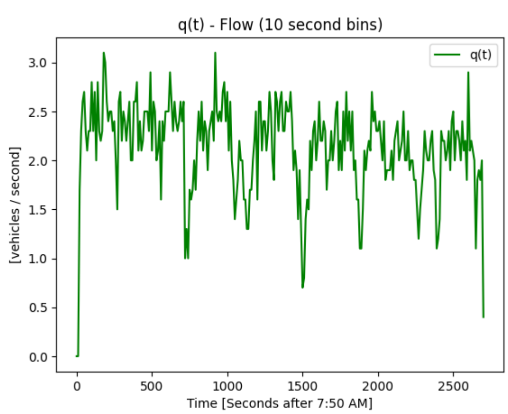

Figure 8. $q(t)$, the out flow rate, the rate of vehicles exiting over 10 second intervals.

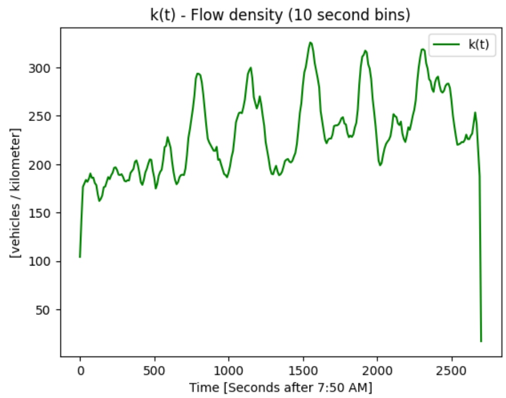

Figure 9. $k(t)$, the flow density, the average density of vehicles over 10 second intervals.

Figure 10 shows the 270 ($k(t)$, $q(t)$) 10 second interval points, and the fitted Daganzo-Newell flux function. The fitted values for the parameters were: α = 0.1141 vehicles / sec, λ = 60.40, and p = 0.2324. Our parameter values are of the same order as the values for the two flux functions in (12).

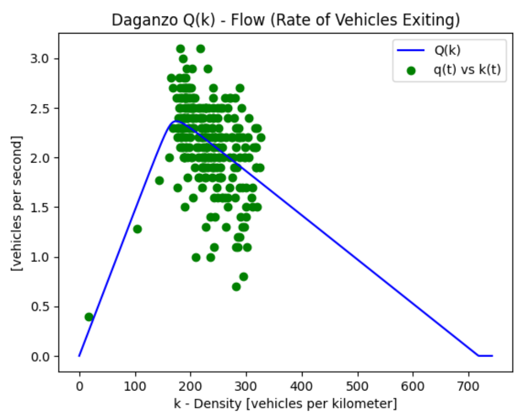

Figure 10. The fitted Daganzo-Newell flux function and the data points used for fitting. Q_{max} is approximately 2.37 vehicles per sec when k is approximately 174 vehicles per km.

The fitted Daganzo-Newell flux function splits relatively evenly the cloud of data points. The data set has very few data points at very low densities, but the curve does fall in between the available points. Our set of empirical data points has a similar distribution as other empirical data points as reported in Figure 1 of (13), Figure 1 of (14), and Figure 2 of (15).

For later comparative evaluation of the models, Figure 11 shows the Greenshields flux function and the set of ($k(t)$, $q(t)$) 10 second interval points.

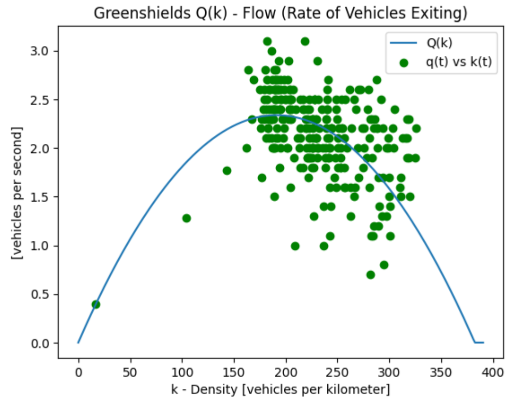

Figure 11. Greenshields flux function and the $(k(t), q(t))$ data points.

Figures 12, 13 and 14 display $u(t)$ at 1 second intervals, $u(t)$ at 10 second intervals, and $empirical\ N(t)$. $u(t)$ at 1 second intervals and $empirical\ N(t)$ are both used in the simulations of the models.

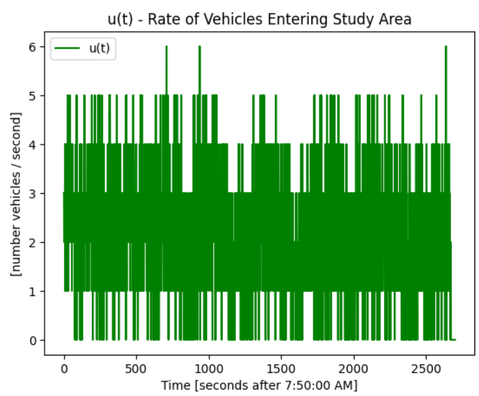

Figure 12. $u(t)$, the rate at which vehicles are entering the study area averaged over 1 second time intervals. u(t) appears remarkably different from $v(t), k(t)$, and $empirical\ N(t)$. However, all four are step functions. The apparent difference is due to the scale of the graph of $u(t)$. The range of $u(t)$, [0, 6], is small compared to the ranges of the other functions.

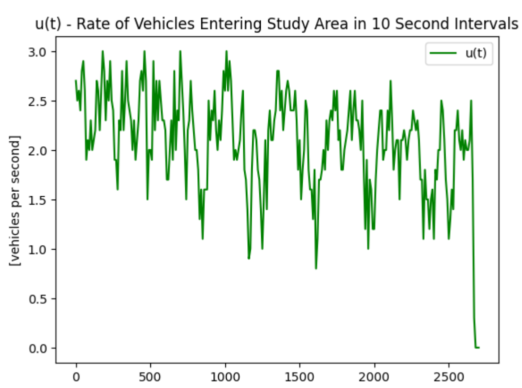

Figure 13. $u(t)$ averaged over 10 second intervals. As to be expected, $u(t)$ averaged over a longer interval is more interpretable visually.

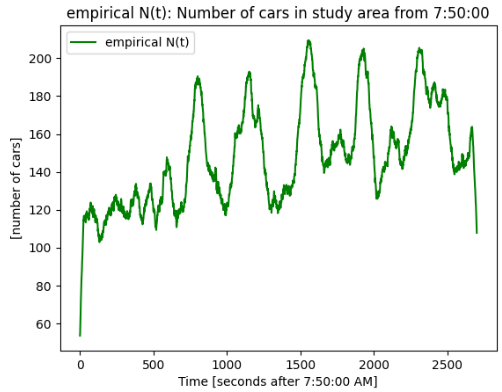

Figure 14. $empirical\ N(t)$, the number of vehicles in the study area.

$empirical\ N(t)$ provided the initial value for predicted $N(t)$ at the starting time of the numerical integration of equation 4. It is observed that the $empirical\ N(t)$ values at 7:50:00 AM and 7:51:00 AM are $empirical\ N(0) = 53.5, empirical\ N(60) = 114.7,$ respectively. For both models, the results of two numerical simulations are presented. The first is for the time period [7:50:00, 8:35:00]. The second is for the time period [7:51:00, 8:35:00]. The initial values for $predicted\ N(t)$ for each simulation were set to equal the observed $empirical\ N(0)$ and $empirical\ N$ (60) respectively.

The results of two sets of numerical presentations were presented for two reasons. First, outliers in the first minute of the data were intentionally omitted when calculating the relationship between $v(t)$ to $k(t)$ for estimating the Greenshields parameters. Second, not all vehicles in the study area were recorded in the first minute, since there were vehicles in the study area prior to 7:50:00 that were not recorded. By 7:51:00, all the vehicles that had entered the study prior to 7:50:00 had exited, and every vehicle in the study area had been tracked as it had entered it. Thus, the second simulation starting the numerical integration at $t = 60$ [7:51:00] is a more accurate simulation. The simulation starting at 7:50:00 is presented primarily for completeness' sake, not for analytical purposes.

Simulation Results for [7:50:00, 8:35:00]

First the simulation results for the Greenshields model are presented in Figures 15 and 16. Figure 15 shows the Greenshields $predicted\ N(t)$ for the time period [7:50:00, 8:35:00].

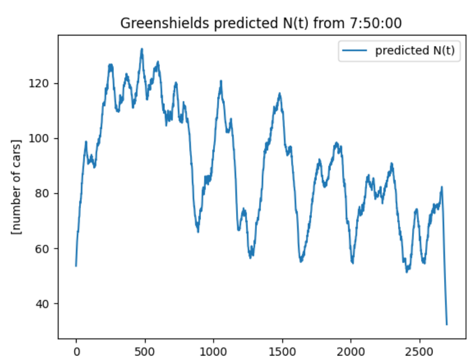

Figure 15. $predicted\ N(t)$, the number of vehicles in the study area predicted by the Greenshields model.

How accurately $predicted\ N(t)$ matched $empirical\ N(t)$ was evaluated by calculating an error function over the time period (eq8). To quantitatively measure how accurate $predicted\ N(t)$ was for a simulation, the following average error was calculated, (eq9), where $t0$ is the start time of a simulation, either 0 or 60 seconds. T is the end time of a simulation, 2,700 seconds. Thus, $(T - t0)$ is the time duration of a simulation. Figure 16 combines the Greenshields $predicted\ N(t)$, the $empirical\ N(t)$, and $error(t)$.

$$error(t) = empirical\ N(t) - predicted\ N(t) \quad \text{(eq8)}$$

$$E = \frac{1}{T-t0}\int_{t0}^{T}|error(t)|\, dt \quad \text{(eq9)}$$

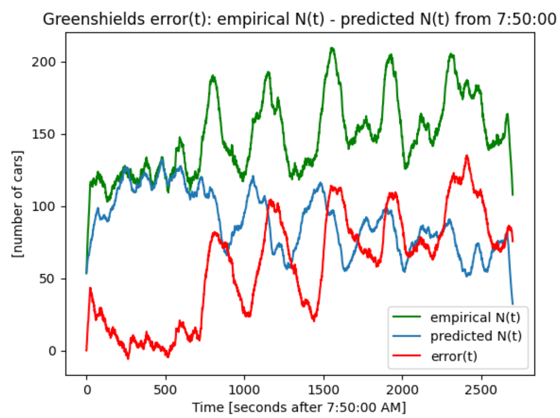

Figure 16. $error(t)$(see equation 8), $empirical\ N(t)$, and $predicted\ N(t)$ for the time period [7:50:00, 8:35:00] for the Greenshields model. The E[Greenshields, 7:50:00 - 8:35:00] = 58.80.

Figures 17 and 18 present the simulation results for the Daganzo-Newell model.

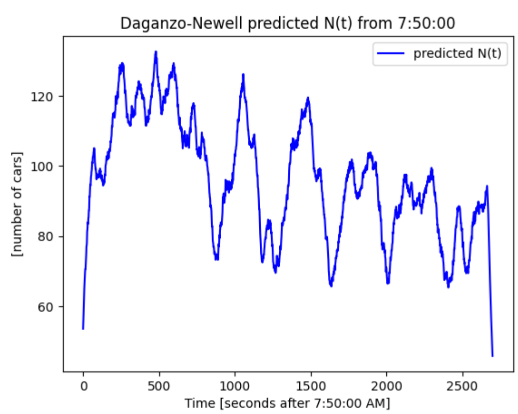

Figure 17. $predicted\ N(t)$, the number of vehicles in the study area predicted by the Daganzo-Newell model.

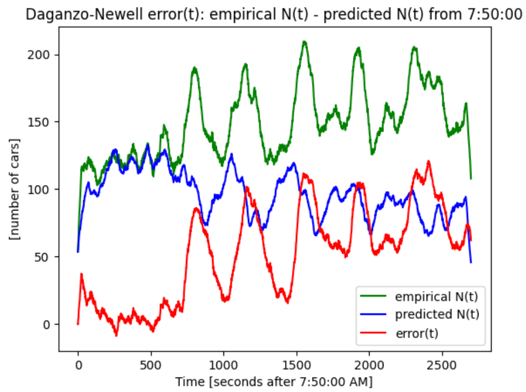

Figure 18. $error(t)$(see equation 8), $empirical\ N(t)$, and $predicted\ N(t)$ for the time period [7:50:00, 8:35:00] for the Daganzo-Newell model. The E[Daganzo-Newell, 7:50:00 - 8:35:00] = 51.99.

Simulation Results for [7:51:00, 8:35:00]

Figure 19 depicts the $empirical\ N(t)$ over the time period [7:51:00, 8:35:00]

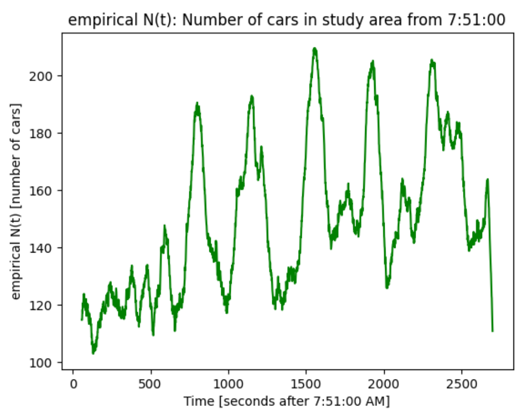

Figure 19. $empirical\ N(t)$ for [7:51:00 AM, 8:35:00 AM].

Figures 20 and 21 present the simulation results for the Greenshields model for time period [7:51:00, 8:35:00].

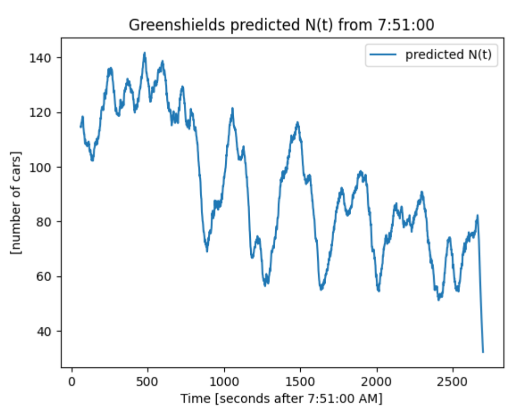

Figure 20. Greenshields model $predicted\ N(t)$ for [7:51:00 AM, 8:35:00 AM].

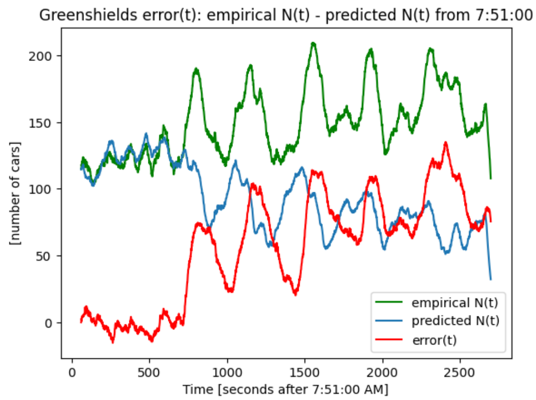

Figure 21. $error(t)$(see equation 8), $empirical\ N(t)$, and $predicted\ N(t)$ for the Greenshields model for the time period [7:51:00, 8:35:00]. The E[Greenshields, 7:51:00 - 8:35:00] = 56.65.

Figures 22 and 23 present the simulation results for the Daganzo-Newell model for time period [7:51:00, 8:35:00].

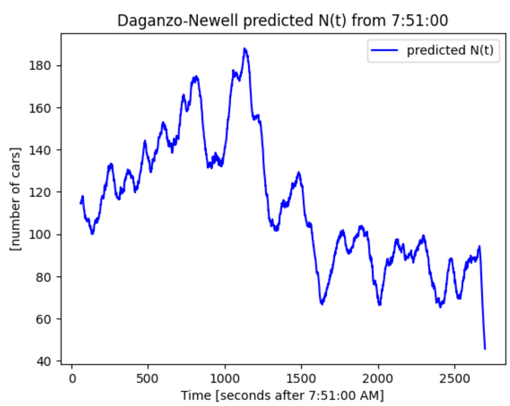

Figure 22. Daganzo-Newell model $predicted\ N(t)$ for [7:51:00 AM, 8:35:00 AM].

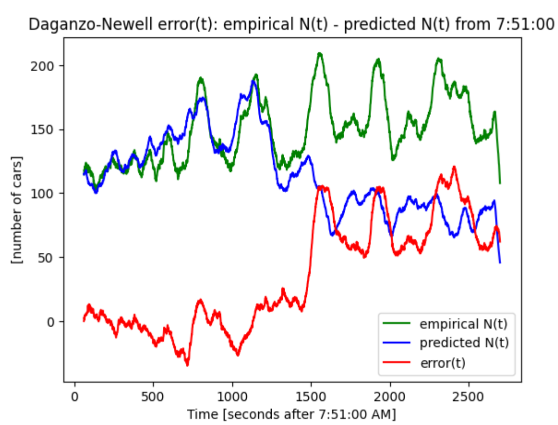

Figure 23. $error(t)$(see equation 8), $empirical\ N(t)$, and $predicted\ N(t)$ for the Daganzo-Newell model for the time period [7:51:00, 8:35:00]. The E[Daganzo-Newell, 7:51:00 - 8:35:00] = 40.47.

For both models, the $predicted\,N(t)$ eventually underpredicted the $empirical\,N(t)$. Generally, both models started out tracking the empirical data for an initial period of time, but then underpredicted for the remainder of the observation period. All the $predicted\,N(t)$'s shared matching similar features as the empirical data, such as local maximums and minimums. For the [7:50:00, 8:35:00] simulations, both models' $predicted\,N(t)$ were similar. The models' predictions tracked well to approximately 8:02:00 (700 seconds), but then consistently underpredicted until 8:35:00.

As discussed earlier, the first minute of the data set contained some missing vehicle trajectory data. By 7:51:00, all the vehicles in the study area were being tracked. Thus, the [7:51:00, 8:35:00] simulations are better for evaluating the performance of the models.

In the second set of simulations, the Daganzo-Newell model performed better. It tracked the empirical data until approximately 8:15:00 (1,500 seconds) and then underpredicted for the remainder of the time. The performance of the Greenshields model was almost the same in both simulations.

Discussion

Macroscopic traffic models first aggregate observations of individual vehicles traveling down a stretch of road to treat them as a continuous flow. Next, variables that capture properties of the continuous flow are used to calibrate a flux function, which relates the outflow rate to the density of traffic. Finally the flux function is used to simulate and predict the empirical data using equations 4, 4a, and 4b.

The study area was composed of five lanes, an on ramp, an auxiliary lane, and an off ramp. But, the models aggregated only the observations in the five mainline lanes into a single continuous flow. Variables that quantitatively described properties of a continuous flow could be accurately and consistently calculated from the observations. Also, the intuition for how the variables are related in the ODE are based upon a conservation law, the conservation of volume: If a vehicle enters the road, it will eventually exit the road. This allowed incorporating the time varying empirical data, the influx rate, $u(t)$, into the simulation of the model as a boundary condition. Finally, the model made predictions for the variable $N(t)$ that could be measured from the data set, hence there was a straightforward way to evaluate the predictive accuracy of the model. A limitation of the models was that they did not describe the internal state of the road. A model treats the entire stretch of the study area as being uniform: the density and velocity of the flow of vehicles is uniform across the entire study area. An analysis of the Greenshields flux function is helpful to better understand the model's predictive performance. First, there were physical limits implied by the Greenshields flux function which were too low. From equation 6, the implied k_{max} was 382.81 vehicles/km (615.95 vehicles/mi), or a maximum number of 245 vehicles in the study, when average velocity approached 0. Continuing with our model's assumption that the flow of vehicles was uniform across the study area, that implied 49 vehicles in a mainline lane. The average length of a vehicle from the data set was 4.6425 m (15.2321 ft). Assuming a minimum headway of half a vehicle length, the minimum required distance would be 6.9638 m per vehicle (22.8482 ft per vehicle). That means 341.2262 m (1,119.5632 ft) of a 640 m (2,100 ft) long lane would be occupied. This meant that there was still ~ 299 m (980 ft) of free space in the lane. Alternatively, the average headway of a mainline lane with 49 vehicles is 8.4187 m (27.6218 ft) – almost two car lengths – a distance traveled in 1.71 seconds by a vehicle moving at 17.70 kph (11.00 mph) or 4.92 m/s (16.13 ft/s). (This was the slowest average velocity measured in the data set when there were 212 vehicles in the study area.) Having 33 more vehicles in the study area would not cause traffic to stop. This implied that the k_{max} of 382.81 vehicles/km (615.95 vehicles/mi) was too low.

A second implied limit from our Greenshields flux function was that the maximum average velocity was 87.98 kph (54.67 mph), which would occur when there were very few vehicles in the study area. This is too low since the legal speed limit is 104.61 kph (65 mph) on this relatively straight stretch of the 101 highway (Figure 2). Indeed, there were individual vehicle velocities of 104.57 km per hour (64.98 mi per hour) in the data set. The empirical maximum average velocity should be close to, or possibly slightly higher than the speed limit. For example, consider a time period around 7:00 AM, when density would be very low, and it is daylight. Figure 15 and Figure 20 show that the Greenshields model generally underpredicted the empirical data. The reason for this becomes more evident when $q(t)$ and $Q(k)$ are compared in Figure 11.

From Figure 11, where there are many observations, the Greenshields curve split the "cloud" of points evenly. Second, the data set did not contain observations across a wide range of densities. There were very few observations when the study area presented with low density, free flowing traffic, and no observations of extremely high density traffic. Thus, when making predictions from our model during periods of traffic that are outside the data set, the Greenshields flux function is extrapolating. Notably, the Greenshields flux function predicted higher outflows than what were observed for densities less than ~175 vehicles per km. These insights about the Greenshields flux function suggest why the Greenshields model consistently underpredicted in the simulations.

Both flux functions simulated similar peak outflows as evident from Figures 10 and 11. The Greenshields peak outflow was 2.34 vehicles per sec when k = 191.27 vehicles per km. The Daganzo-Newell peak outflow was 2.37 vehicles per sec when k = 174 vehicles per km. From Figure 18 and Figure 23, the Daganzo-Newell model matched the performance of the Greenshields model for the [7:50:00, 8:35:00] simulation. But, the Daganzo-Newell performed better than the Greenshields for the [7:51:00, 8:35:00] simulation. From examining Figure 10, the Daganzo-Newell flux function split the cloud of data points evenly. Also, at lower densities, the Daganzo-Newell curve was closer to the few available data points. Unlike the Greenshields function, the Daganzo-Newell flux function was not symmetric. Although not identical, the Greenshields and the Daganzo-Newell models presented with similar underpredictions in the [7:50:00, 8:35:00] simulations. This was not completely unexpected, since both flux functions were similar. However, because the first 60 seconds of the data set contained incomplete vehicle trajectory data, explanatory hypothesis was not possible. For the [7:51:00, 8:35:00] simulation, the Daganzo-Newell model simulated the observed data better, although after ~ 1,500 seconds it also underpredicted. A traffic flux function does not fully capture the complexity of real traffic flow. Past a critical density, there are many observed outflow values for a given density – $q(t)$ is not a function of $k(t)$. (The "cloud" of data points in Figure 10 and

Figure 11). However, relatively, the Daganzo-Newell model performed better than the Greenshields model.

There are various methods to improve on the models presented in this study. A first path would be to collect additional observations of traffic in the study area during a different time of the day, in particular, during a period of low traffic density. For example, early in the morning after sunrise ~ 7:00 AM. This would provide additional empirical data points that could be incorporated into calculating more accurate relationships between $v(t), q(t)$, and $k(t)$, potentially improving the predictive accuracy of the models.

A second path would be to improve the mathematical modeling of the macroscopic variables, e.g., $v(t)$, $q(t)$, $k(t)$, $u(t)$, $empirical\, N(t)$. In this paper's work, the functions for these variables were calculated as step functions, averages of values over time and intervals. The traffic flux functions are continuous and the numerical simulations are performed effectively in continuous time. Methods to calculate the macroscopic variables as continuous functions would be more realistic than if calculated as step functions. It would be worthwhile to investigate methods to calculate continuous "averages" for the empirical variables.

Finally, the empirical data provided detailed location information about the vehicles inside the study area. Given this, it should be possible to build a model that includes spatial dependence inside the study area. Thus, the ODE model of equation 4, which utilizes variables of time, flow, and volume would become a PDE that utilizes variables of time, flow, location, and density. This more sophisticated model is the Lighthill-Whitham-Richards (LWR) traffic model.

Conclusion

The NGISM traffic data set (11) provided vehicle trajectory information in great detail and accuracy – spatially and temporally – for a stretch of US 101 highway in Los Angeles. This allowed detailed traffic modeling, simulation, and validation. Two different ordinary differential equation based macroscopic models of traffic flow were constructed to model traffic flow. The models were constructed using the Greenshields and the Daganzo-Newell traffic flux functions.

Using a part of the data set, the flux functions' parameter values were estimated. Analysis of the flux functions was performed by calculating physical limits implied by them and evaluating how realistic those implied limits were. Then using a different part of the data set, the models were simulated numerically. Both the flux functions and the simulations were analyzed for how realistically they reconstructed the data. The simulation results showed that the Daganzo-Newell model was more accurate than the Greenshields at predicting the observed data.

References

1. Pravin, V. (2005). Reducing Highway Congestion: An Empirical Approach. *European Journal of Control.* 11:301–309. https://doi.org/10.3166/ejc.11.301-309

2. Lighthill, M. J., & Whitham, G. B. (1955). On Kinematic Waves. II. A Theory of Traffic Flow on Long Crowded Roads. *Proceedings of the Royal Society of London. Series A, Mathematical and Physical Sciences*, *229*(1178), 317–345. http://www.jstor.org/stable/99769

3. Richards, P. I. (1956). Shock Waves on the Highway. *Operations Research*, *4*(1), 42–51. http://www.jstor.org/stable/167515

4. Godunov, S. K. (1959). A difference scheme for numerical computation of discontinuous solutions of equations of fluid dynamics. *Math. Sb*., 47:271 – 290.

5. McCartney, M., & Carey, M. (1999). Modelling Traffic Flow: Solving and Interpreting Differential Equations. *Teaching Mathematics and Its Applications: International Journal of the IMA*, 18(3), 115-121. https://doi.org/10.1093/teamat/18.3.115

6. Greenshields, B.D. (1935). A study of traffic capacity. *Proceedings of the Highway Research Record*, 14:448–477.

7. Daganzo, C., (1994). The cell transmission model: A dynamic representation of highway traffic consistent with the hydrodynamic theory, *Transportation Research Part B: Methodological*, Volume 28, Issue 4, 1994, Pages 269-287, ISSN 0191-2615, https://doi.org/10.1016/0191-2615(94)90002-7

8. Daganzo, C., & Geroliminis, N., (2008). An analytical approximation for the macroscopic fundamental diagram of urban traffic, *Transportation Research Part B: Methodological*, Volume 42, Issue 9, 2008, Pages 771-781, ISSN 0191-2615, https://doi.org/10.1016/j.trb.2008.06.008

9. Wageningen-Kessels, F., Lint, H., Vuik, K., & Hoogendoorn, S. (2015). Genealogy of traffic flow models, *EURO Journal on Transportation and Logistics*, Volume 4, Issue 4, 2015, Pages 445-473, ISSN 2192-4376, https://doi.org/10.1007/s13676-014-0045-5

10. Bramich, D. M., Menéndez, M., & Ambühl, L. (2022). Fitting Empirical Fundamental Diagrams of Road Traffic: A Comprehensive Review and Comparison of Models Using an Extensive Data Set, *IEEE Transactions on Intelligent Transportation Systems*, vol. 23, no. 9, pp. 14104-14127, Sept. 2022, http://doi.org/10.1109/TITS.2022.3142255

11. U.S. Department of Transportation Federal Highway Administration (2016). *Next Generation Simulation (NGSIM) Vehicle Trajectories and Supporting Data* [Data set]. ITS DataHub. http://doi.org/10.21949/1504477

12. Fan, S., & Seibold, B. (2013). Data-Fitted First-Order Traffic Models and Their Second-Order Generalizations: Comparison by Trajectory and Sensor Data. *Transportation Research Record*, 2391(1), 32-43. https://doi.org/10.3141/2391-04

13. Geroliminis, N; Daganzo, CF (2008). Existence of urban-scale macroscopic fundamental diagrams: Some experimental findings. *Transportation Research Part B: Methodological,* Volume 42, Issue 9, p759-p770. https://doi.org/10.1016%2Fj.trb.2008.02.002

14. Amirgholy, M. & Shahabi, M. & Gao, H. (2017). Optimal design of sustainable transit systems in congested urban networks: A macroscopic approach. *Transportation Research Part E: Logistics and Transportation Review*. 103. 261-285. https://doi.org/10.1016/j.tre.2017.03.006

15. Anuar, K.A., Habtemichael, F.G., & Cetin, M. (2015). Estimating Traffic Flow Rate on Freeways from Probe Vehicle Data and Fundamental Diagram. *2015 IEEE 18th International Conference on Intelligent Transportation Systems*, 2921-2926. https://doi.org/10.1109/ITSC.2015.468

16. Khoudari, N., Seibold, B. (2023). Multiscale Properties of Traffic Flow: The Macroscopic Impact of Traffic Waves. In: Booß-Bavnbek, B., Hesselbjerg Christensen, J., Richardson, K., Vallès Codina, O. (eds) Multiplicity of Time Scales in Complex Systems. Mathematics Online First Collections. Springer, Cham. https://doi.org/10.1007/16618_2022_38

17. Ni, D. (2016). Ch. 5 - Conservation Law. *Traffic Flow Theory: Characteristics, Experimental Methods, and Numerical Techniques.* p75-p85. https://doi.org/10.1016/B978-0-12-804134-5.00005-2

18. Lu, X.Y., Varaiya, P., Horowitz, R., (2009). Fundamental Diagram Modelling and Analysis Based NGSIM Data, *IFAC Proceedings Volumes*, Volume 42, Issue 15, 2009, Pages 367-374, ISSN 1474-6670, ISBN 9783902661500, https://doi.org/10.3182/20090902-3-US-2007.0068.